CrossMark

ORIGINAL ARTICLE

Cubic-RBF-ARX modeling and model-based optimal setting control in head and tail stages of cut tobacco drying process

Feng Zhou[1,2] · Hui Peng[1,2] · Wenjie Ruan[1,3] · Dan Wang[1,2] · Mingyue Liu[1,2] · Yunfeng Gu[1,2] · Li Li[1,2]

Abstract This paper presents a data-driven modeling technique used to build a multi-sampling-rate RBF-ARX (MSR-RBF-ARX) model for capturing and quantifying global nonlinear characteristics of the head and tail stage drying process of a cylinder-type cut tobacco drier. In order to take full account of influence of the input variables to outlet cut tobacco moisture content in whole drying process, and meanwhile, to avoid orders of the model too large, this paper designs a special MSR-RBF-ARX model structure that incorporates the advantages of parametric model and nonparametric model in nonlinear dynamics description for the process. Considering this industrial process identification problem, a hybrid optimization algorithm is proposed to identify the MSR-RBF-ARX model using the multi-segment historical data set in different seasons and working conditions. To obtain better long-term forecasting performance of the model, a long-term forecasting performance index is introduced in the algorithm. To accelerate the computational convergence, in the hybrid algorithm, one-step predictive errors of the model are minimized first to get a set of the model parameters that are just used as the model initial parameters, and then, the model parameters are further optimized by minimizing long-term forecasting errors of the model. Based on the estimated model, a set of optimal setting curves of the input variables are obtained by optimizing parameters of the designed input variable models. The effectiveness of the proposed modeling and setting control strategy for the process are demonstrated by simulation studies.

Keywords Cubic-RBF-ARX model · Cut tobacco drying process · Optimal setting control · Optimization method

1 Introduction

Cut tobacco drying process is the most important part of cigarette producing process [1, 2]. The moisture content of dried cut tobacco will directly affect final cigarette quality. The main function of a cut tobacco dryer is to make the moisture content of dried cut tobacco be controlled in a certain range, so as to satisfy the technical requirements. According to the production process and technology, the drying process of a cylinder-type cut tobacco dryer can be divided into three stages: head, middle and tail stages. This paper mainly studies modeling and control problems in head and tail stage drying process of a cylinder-type cut tobacco dryer using data-driving identification approach.

Control in head and tail stage of the cut tobacco drying process is very difficult, because this process is multivariable, overactuated, strong coupling, large time delay and lack of important measuring variable, i.e., outlet or inlet cut tobacco moisture content in head or tail dying process, this means that the general feedback control approaches are not able to be used to the process control. At present, the main way is manual setting control by experience [3], or using

✉ Hui Peng
huipeng@mail.csu.edu.cn

Feng Zhou
sir0501@live.cn

1 School of Information Science and Engineering, Central South University, Changsha 410083, Hunan, China

2 Collaborative Innovation Center of Resource-conserving and Environment-friendly Society and Ecological Civilization, Changsha 410083, Hunan, China

3 School of Computer Science, University of Adelaide, Adelaide, SA 5005, Australia

setting control of some process variables based on a theoretical model [4, 5], which was built on the basis of heat and mass balance of the materials in the drying process. Usually, the control performance is not good, and it results in lots of over-dried cut tobacco in the process due to inaccuracy of the model [6]. Spraying water in these two stages may reduce over-dried cut tobacco, but actually it can only make surface moisture of outlet cut tobacco enlarge while does nothing to improve inner quality of cut tobacco. In addition, it also adds difficulty to control of the drying process.

Theoretical model is usually very complicated, although it may be precise [7]. Some methods were proposed to approximate the nature behavior of a nonlinear system in the literature. The most common way is to build a simplified model of system under some assumptions [7]. Even so, some parameters of the simplified theoretical model may be still unknown or difficult to be obtained through the system physical structure. In fact, if the historical data of a plant can be obtained, it is advisable to apply a data-driving approach [8] for building an identification model of the system. Actually, a large number of industrial processes may be regarded as systems having time-varying working-points and may be locally linearized at each working-point. As a class of special coefficient-varying regressive models, the radial basis function neural network-based state-dependent autoregressive model (RBF-ARX) [9] has been studied in several years. Structure of RBF-ARX model and its parameters optimization method (SNPOM, structured nonlinear parameters optimization method) was first proposed in Ref. [9]. As noted by Haggan et al. [10], an important property of RBF-ARX models, compared with the most other coefficient-varying models, is that this type of models incorporated the advantages of the RBF neural network in function approximation and the state-dependent autoregressive models (SD-ARX) in nonlinear dynamics description. Over the past decade, the RBF-ARX modeling and the model-based control have been studied in nonlinear NOx decomposition process in a thermal power plant [10–12], water tank system control [13], ship's tracking control [14], magnetic levitation system control [15] and quadrotor attitude control [16], etc.

This paper presents a data-driven modeling technique that is used to build a multi-sampling-rate RBF-ARX (MSR-RBF-ARX) model for capturing and quantifying the global nonlinear characteristics of the head and tail stage drying process of a cylinder-type cut tobacco drier. The MSR-RBF-ARX model is a hybrid model, which incorporates the advantages of parametric model and nonparametric model in nonlinear dynamics description. Designing this model is because in head and tail stages of the cut tobacco drying process, the cut tobacco that just enters into the dryer actually has obvious influence on the entire cut tobacco drying process. In order to take full account of influence of the input variables in whole drying process on the outlet cut tobacco moisture content and, meanwhile, to avoid orders of the model too large, this paper, for the first time, separately designs a MSR-RBF-ARX model structure for modeling the head or tail drying process. Through comparison of several model structures, it is verified that the MSR-RBF-ARX model with Cubic function-type base function, namely MSR-Cubic-RBF-ARX model can better represent global characteristics of the head or tail stage drying process.

Considering this special industrial process identification problem, the multi-segment historical data set in different seasons and working conditions is used as identification data of the drying process models, and a hybrid optimization algorithm is designed to identify the MSR-Cubic-RBF-ARX model using multi-segment historical data. In order to obtain better long-term forecasting performance of the model, a long-term forecasting performance index is introduced in the algorithm. To accelerate the computational convergence, in the hybrid algorithm, one-step predictive errors of the MSR-Cubic-RBF-ARX model are minimized first to get a set of the model parameters that are just used as the model initial parameters, and then, the model parameters are further optimized by minimizing long-term forecasting errors of the model. The purpose of modeling the drying process is to design a set of optimal setting variables of the process to make over-dried cut tobacco in the head and tail drying process as few as possible. To this end, we designed a double-S-type curve as basic structure of some process variables, and based on the estimated MSR-Cubic-RBF-ARX model, a set of optimal setting curves of the input variables are obtained by optimizing parameters of the setting variable curves. The effectiveness of the proposed modeling and setting control strategy are demonstrated by simulation studies.

2 Cut tobacco drying process modeling by MSR-Cubic-RBF-ARX model

Structure diagram of a typical cylinder-type cut tobacco dryer is depicted in Fig. 1. In a drying process, the head stage starts when the inlet cut tobacco flow is first detected and ends till the moisture content of outlet cut tobacco can be measured. The process after the head stage is a long time middle stage. After the middle stage, the tail stage begins when the inlet cut tobacco flow changes from a normal value to zero.

From Fig. 1, one can see that the inlet cut tobacco flow u_4 (kg/h) can be detected before cut tobacco enters the dryer. After the time of T_1, cut tobacco arrives at measuring point of the inlet cut tobacco moisture content u_5 (%) and, then, goes into the cylinder after the time of T_2. After the

Fig. 1 Structure diagram of cylinder-type cut tobacco dryer
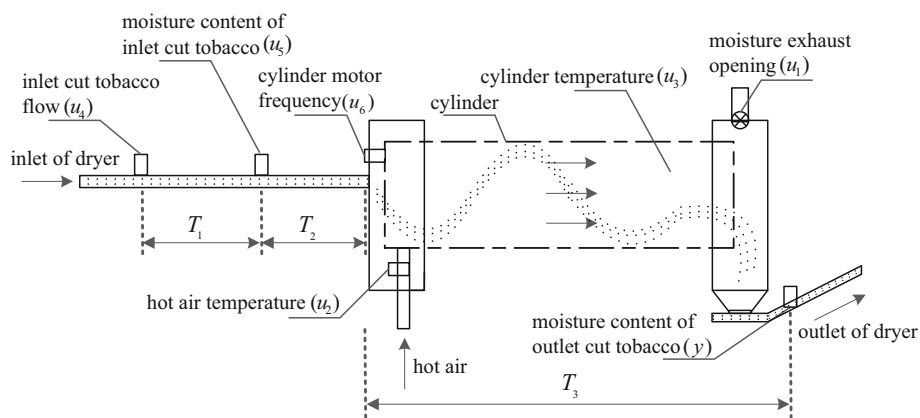
time of T_3, the dried cut tobacco goes out of the cylinder and the moisture content of outlet cut tobacco y (%) can be detected. This process will take a long period from where the inlet cut tobacco flow u_4 is first detected to where the outlet cut tobacco moisture content y can be first measured. For the dryer studied in this paper, the processing time is about 5 min. The other main variables affecting the drying process are the moisture exhaust opening u_1 (%), the hot air temperature u_2 (°C), the cylinder temperature u_3 (°C) and the cylinder motor frequency u_6 (Hz).

In head stage of the drying process, cut tobacco entering the dryer keeps increasing while there is no measuring value of outlet cut tobacco, so one cannot use feedback control approach to the outlet cut tobacco moisture content. In tail stage of the drying process, there is no inlet cut tobacco flow, and the drying cylinder has a large heat capacity that results in slow decline of temperature of the drying cylinder. Therefore, as mentioned before, existing control methods may be not satisfactory and easily lead to lots of over-dried cut tobacco in head and tail drying process. In this section, a multi-sampling-rate Cubic-RBF-ARX (MSR-Cubic-RBF-ARX) modeling method is proposed to represent the dynamic behavior of the head and tail stage processes separately, and the model-based optimal setting control strategy is then designed to control the two stage processes in Sect. 3.

2.1 Construction of MSR-Cubic-RBF-ARX model

Consider a multivariable nonlinear and non-stationary system, which can be represented by the following discrete time nonlinear ARX model:

$$y(t) = f(y(t-1), \ldots, y(t-k_a), u(t-1), \ldots, u(t-k_b)) + \xi(t) \tag{1}$$

where $y(t) \in \Re^n$ denotes the output, $u(t) \in \Re^h$ denotes the input and $\{\xi(t) \in \Re^n\}$ denotes the white noise sequence with zero mean; $f(\cdot)$ denotes a nonlinear structure; k_a and k_b denote the corresponding orders. Actually, a large number of industrial processes may be regarded as systems having time-varying working-points [9]. In this situation, the state-dependent ARX model [17] may be adapted to approximate the nonlinear structure $f(\cdot)$ in (1), and it yields

$$y(t) = \phi_0(w(t-1)) + \sum_{i=1}^{k_a} \phi_{y,i}(w(t-1))y(t-i)$$
$$+ \sum_{i=1}^{k_b} \phi_{u,i}(w(t-1))u(t-i) + \xi(t) \tag{2}$$

where $\phi_0(w(t-1))$, $\phi_{y,i}(w(t-1))$ and $\phi_{u,i}(w(t-1))$ are the state-dependent regressive coefficient matrices of suitable dimensions. $w(t-1)$ is regarded as the working-point variable which has a direct or indirect relationship with the system input or output. If RBF neural networks are selected to approximate the regressive coefficient matrices of model (2), the RBF-ARX model thus can be derived [9], which is rewritten as

$$y(t) = a_{0,t-1} + \sum_{i=1}^{k_a} a_{i,t-1}y(t-i) + \sum_{i=1}^{k_b} b_{i,t-1}u(t-i) + \xi(t),$$

$$\begin{cases} a_{0,t-1} = c_0^y + \sum_{k=1}^{m} c_k^y \varphi\left(\left\|w(t-1) - z_k^y\right\|_2\right), \\ a_{i,t-1} = c_{i,0}^y + \sum_{k=1}^{m} c_{i,k}^y \varphi\left(\left\|w(t-1) - z_k^y\right\|_2\right), \\ b_{i,t-1} = c_{i,0}^u + \sum_{k=1}^{m} c_{i,k}^u \varphi\left(\left\|w(t-1) - z_k^u\right\|_2\right), \\ w(t-1) = \begin{bmatrix} w_1^{\mathrm{T}} & \ldots & w_d^{\mathrm{T}} \end{bmatrix}^{\mathrm{T}}, \\ z_k^j = \begin{bmatrix} z_{k,1}^{j\mathrm{T}} & \ldots & z_{k,d}^{j\mathrm{T}} \end{bmatrix}^{\mathrm{T}}, \quad j = y, u. \end{cases}$$

$$\tag{3}$$

where $a_{0,t-1}$, $\{a_{i,t-1} | i = 1, 2, \ldots, k_a\}$ and $\{b_{i,t-1} | i = 1, 2, \ldots, k_b\}$ are the nonlinear regressive coefficient matrices and vary with the working-point $w(t-1)$; $\varphi(\cdot)$ is nonlinear base function; k_a, k_b, m and d are the corresponding model orders; $\{c_k^y, c_{i,k}^y | k = 0, 1, \ldots, m; \quad i =$

$1, \ldots, k_a\}$ and $\left\{c_{i,k}^u | k = 0, 1, \ldots, m; \quad i = 1, \ldots, k_b\right\}$ are the linear weighting coefficient matrices; $\{z_k^j | k = 1, \ldots, m; \quad j = y, u\}$ are the RBF neural network centers; $\|\cdot\|_2$ means 2-norm matrix; $\xi(t)$ is the modeling error, assuming as Gauss white noise. It is natural to interpret model (3) as a globally nonlinear model in which the evolution of the system is governed by a set of nonlinear regressive coefficient matrices $\{a_{i,t-1}, \quad b_{i,t-1}\}$, and a local mean $a_{0,t-1}$ varying with the 'working-point' of the system. There have been many reports where researches have applied the RBF-ARX modeling to various types of nonlinear systems [11, 13–16]. However, the majority of these researches used Gaussian base function to approximate the state-dependent coefficients of the RBF-ARX model. This may be appropriate in some cases; however, this may not always be optimal in other cases.

In this paper, based on the above RBF-ARX modeling technology and considering the particularities of the head and tail stages in the drying process, an efficient multi-sampling-rate RBF-ARX (MSR-RBF-ARX) model structure is designed for modeling the dynamic characteristics of the two stages separately. The MSR-RBF-ARX model is a kind of hybrid model, which incorporates the advantages of parametric model and nonparametric model in nonlinear dynamics description. The potential base function for the MSR-RBF-ARX model of the head and tail process considered here includes Gauss, Cubic and Multiquadratic base functions [18]. Through comparison of several model

moisture exhaust opening, the hot air temperature and the cylinder driving motor frequency etc. Especially in the head and tail stages, the cut tobacco that just enters into the cylinder actually has obvious influence on the entire cut tobacco drying process. In order to take full account of influence of the input variables in whole drying process on the outlet cut tobacco moisture content and, meanwhile, to avoid the orders of the regressive variables too large, this paper separately designed the MSR-RBF-ARX model structures for modeling the head and tail drying process.

2.1.1 MSR-Cubic-RBF-ARX model of head stage process

The head stage drying process starts when the cut tobacco flow jumps from zero to a value and ends till the moisture content of outlet cut tobacco can be measured. The multi-sampling-rate Cubic-RBF-ARX model structure is designed as follows:

$$
\begin{aligned}
y^h(t) = a_{0,t-1}^h + \sum_{i=1}^{k_a^h} a_{i,t-1}^h y^h(t-i) + \sum_{i=1}^{k_b^h} b_{i,t-1}^{h1} u_1^h\left(t - i \cdot T_0^h\right) \\
+ \sum_{i=1}^{k_b^h} b_{i,t-1}^{h2} u_2^h\left(t - i \cdot T_0^h\right) + \sum_{i=1}^{k_b^h} b_{i,t-1}^{h3} u_3^h\left(t - i \cdot T_0^h\right) \\
+ \sum_{i=1}^{k_b^h} b_{i,t-1}^{h4} u_4^h\left(t - T_1^h - T_2^h - i \cdot T_0^h\right) + \sum_{i=1}^{k_b^h} b_{i,t-1}^{h5} u_5^h \\
\left(t - T_2^h - i \cdot T_0^h\right) + \xi^h(t)
\end{aligned}
$$

(4)

$$
\begin{cases}
a_{0,t-1}^h = c_0^{y^h} + \sum_{k=1}^{m^h} c_k^{y^h}\left(\left\|w^h(t-1) - z_k^{y^h}\right\|_2^3\right), \\
a_{i,t-1}^h = c_{i,0}^{y^h} + \sum_{k=1}^{m^h} c_{i,k}^{y^h}\left(\left\|w^h(t-1) - z_k^{y^h}\right\|_2^3\right), \\
b_{i,t-1}^{h\delta} = c_{i,0}^{u_\delta^h} + \sum_{k=1}^{m^h} c_{i,k}^{u_\delta^h}\left(\left\|w^h(t-1) - z_k^{u^h}\right\|_2^3\right), \quad \delta = 1, 2, 3, 4, 5; \\
w^h(t-1) = \begin{bmatrix} u_4^h(t-1) & \cdots & u_4^h(t-d^h) \\ u_5^h(t-1) & \cdots & u_5^h(t-d^h) \end{bmatrix}^T, \quad z_k^j = \begin{bmatrix} z_{k,1}^{j,1} & \cdots & z_{k,d^h}^{j,1} \\ z_{k,1}^{j,2} & \cdots & z_{k,d^h}^{j,2} \end{bmatrix}^T, \quad j = y^h, u^h; \\
T_1^h = \lfloor T_1/T \rfloor, \quad T_2^h = \lfloor T_2/T \rfloor, \quad T_0^h = \lfloor T_3/(T \cdot k_b^h) \rfloor.
\end{cases}
$$

(5)

structures, it is verified that the multi-sampling-rate RBF-ARX model with Cubic function-type base function (MSR-Cubic-RBF-ARX) can better represent the global characteristics of the head or tail stage drying process.

In the drying process, to dry cut tobacco in the cylinder needs a long time (about 5 min), and the moisture content of outlet cut tobacco depends on the inlet cut tobacco flow and moisture content, the cylinder temperature, the

where $y^h(t)$ is the moisture content of outlet cut tobacco in the head stage; $u_\delta^h(t)$ $(\delta = 1, 2, 3, 4, 5)$ are the input variables, which are the moisture exhaust opening u_1 (%), the hot air temperature u_2 (°C), the cylinder temperature u_3 (°C), the inlet cut tobacco flow u_4 (kg/h) and the moisture content of inlet cut tobacco u_5 (%) in the head stage, respectively; $a_{0,t-1}^h$, $\left\{a_{i,t-1}^h | i = 1, \ldots, k_a^h\right\}$ and

$\{b_{i,t-1}^{h\delta}|i=1,\ldots,k_b^h; \quad \delta=1,2,3,4,5\}$ are the nonlinear regressive coefficient matrices varying with the working-point $w^h(t-1)$; Considering the dynamic characteristics of the head stage drying process, this paper takes the inlet cut tobacco flow u_4 and the moisture content of inlet cut tobacco u_5 as the working-point state; k_a^h, k_b^h, m^h and d^h are the orders of the model; $\left\{c_k^{y^h}, c_{i,k}^{y^h}|k=0,1,\ldots,m^h; \quad i=1,\ldots,k_a^h\right\}$ and $\left\{c_{i,k}^{u_\delta^h}|k=0,1,\ldots,m^h; \quad i=1,\ldots,k_b^h; \quad \delta=1,2,3,4,5\right\}$ are the linear weighting coefficient matrices; $\left\{z_{k,g}^{j,1}, z_{k,g}^{j,2}|k=1,\ldots,m^h; \quad j=y^h, u^h; \quad g=1,\ldots,d^h\right\}$ are the RBF neutral network centers; $\xi^h(t)$ is the modeling error, assuming as the Gauss white noise; T is the sample period of the drying process; T_1^h and T_2^h are the available time delay of head stage drying process; T_3^h is the duration time step of the cut tobacco in the cylinder during the head stage drying process; $\lfloor\cdot\rfloor$ in (5) means rounded down integer arithmetic. As shown in model (4), the sampling period of the input variables in the model is $T_0^h=\lfloor T_3/(T\cdot k_b^h)\rfloor$ times of sampling period of the output variable $y^h(t)$.

2.1.2 MSR-Cubic-RBF-ARX model of tail stage process

When the inlet cut tobacco flow changes from a normal value to zero, the tail stage drying process starts, and in this stage, there is no inlet cut tobacco flow measuring signal. The multi-sampling-rate Cubic-RBF-ARX model structure of the tail stage is designed as follows:

$$
\begin{aligned}
y^e(t) =\ & a_{0,t-1}^e + \sum_{i=1}^{k_a^e} a_{i,t-1}^e y^e(t-i) + \sum_{i=1}^{k_b^e} b_{i,t-1}^{e1} u_1^e\left(t-i\cdot T_0^e\right) \\
& + \sum_{i=1}^{k_b^e} b_{i,t-1}^{e2} u_2^e\left(t-i\cdot T_0^e\right) + \sum_{i=1}^{k_b^e} b_{i,t-1}^{e3} u_3^e\left(t-i\cdot T_0^e\right) \\
& + \sum_{i=1}^{k_b^e} b_{i,t-1}^{e4} u_4^e\left(t-T_1^e-T_2^e-i\cdot T_0^e\right) + \sum_{i=1}^{k_b^e} b_{i,t-1}^{e5} u_5^e \\
& \times \left(t-T_2^e-i\cdot T_0^e\right) + \sum_{i=1}^{k_b^e} b_{i,t-1}^{e6} u_6^e\left(t-i\cdot T_0^e\right) + \xi^e(t)
\end{aligned}
\tag{6}
$$

where $y^e(t)$ is the output that is the moisture content of outlet cut tobacco in the tail stage; $u_\delta^e(t)$ ($\delta=1,2,3,4,5,6$) are the input variables, namely the moisture exhaust opening u_1 (%), the hot air temperature u_2 (°C), the cylinder temperature u_3 (°C), the inlet cut tobacco flow u_4 (kg/h), the moisture content of inlet cut tobacco u_5 (%) and the cylinder motor frequency u_6 (Hz) in the tail stage, respectively; $a_{0,t-1}^e$, $\left\{a_{i,t-1}^e|i=1,\ldots,k_a^e\right\}$ and $\left\{b_{i,t-1}^{e\delta}|i=1,\ldots,k_b^e; \quad \delta=1,2,3,4,5,6\right\}$ are the nonlinear regressive coefficient matrices varying with the working-point $w^e(t-1)$; Considering the dynamic characteristics of the tail stage, this paper takes the hot air temperature u_2 and the cylinder motor frequency u_6 as the working-point state variable; k_a^e, k_b^e, m^e and d^e are the orders of the model; $\left\{c_k^{y^e}, c_{i,k}^{y^e}|\ k=0,1,\ldots,m^e; \quad i=1,\ldots,k_a^e\right\}$ and $\left\{c_{i,k}^{u_\delta^e}|k=0,1,\ldots,m^e; \quad i=1,\ldots,k_b^e; \quad \delta=1,2,3,4,5,6\right\}$ are the linear weighting coefficient matrices; $\left\{z_{k,g}^{j,1}, z_{k,g}^{j,2}|k=1,\ldots,m^e; \quad j=y^e, u^e; \quad g=1,\ldots,d^e\right\}$ are the RBF neutral network centers; $\xi^e(t)$ is the modeling error, assuming as the Gauss white noise; T is the sample period of the drying process; T_1^e and T_2^e are the available time delay of the tail stage drying process; T_3^e is the duration time step of the cut tobacco in the cylinder during the tail stage drying process; $\lfloor\cdot\rfloor$ in (7) means rounded down integer arithmetic; Similar to model (4) of the head stage, in MSR-Cubic-RBF-ARX model (6) of the tail stage, the sampling period of input variables is $T_0^e=\lfloor T_3/(T\cdot k_b^e)\rfloor$ times of sampling period of the output variable $y^e(t)$.

2.2 Hybrid optimization algorithm for estimation of MSR-Cubic-RBF-ARX model

Identification of a RBF-ARX model includes estimating structure and parameters of the model. In the previous work, the structured nonlinear parameter optimization method (SNPOM) [9, 11] was proposed to identify all parameters of a RBF-ARX model by minimizing one-step-ahead predictive errors of the model. The SNPOM

$$
\begin{cases}
a_{0,t-1}^e = c_0^{y^e} + \sum_{k=1}^{m^e} c_k^{y^e}\left(\left\|w^e(t-1)-z_k^{y^e}\right\|_2^3\right), \\[2mm]
a_{i,t-1}^e = c_{i,0}^{y^e} + \sum_{k=1}^{m^e} c_{i,k}^{y^e}\left(\left\|w^e(t-1)-z_k^{y^e}\right\|_2^3\right), \\[2mm]
b_{i,t-1}^{e\delta} = c_{i,0}^{u_\delta^e} + \sum_{k=1}^{m^e} c_{i,k}^{u_\delta^e}\left(\left\|w^e(t-1)-z_k^{u^e}\right\|_2^3\right), \quad \delta=1,2,3,4,5,6; \\[2mm]
w^e(t-1) = \begin{bmatrix} u_2^e(t-1) & \cdots & u_2^e(t-d^e) \\ u_6^e(t-1) & \cdots & u_6^e(t-d^e) \end{bmatrix}^{\mathrm{T}}, \quad z_k^j = \begin{bmatrix} z_{k,1}^{j,1} & \cdots & z_{k,d^e}^{j,1} \\ z_{k,1}^{j,2} & \cdots & z_{k,d^e}^{j,2} \end{bmatrix}^{\mathrm{T}}, \quad j=y^e, u^e; \\[2mm]
T_1^e = \lfloor T_1/T\rfloor, T_2^e = \lfloor T_2/T\rfloor, T_0^e = \lfloor T_3/(T\cdot k_b^e)\rfloor.
\end{cases}
\tag{7}
$$

estimates the model's nonlinear and linear parameters iteratively and separately, which uses the Levenberg–Marquardt method (LMM) to estimate the nonlinear parameters and uses the Least-Squares method (LSM) to estimate the linear parameters. Based on this idea, some other training algorithms, such as a global–local optimization approach [19, 20], a variable projection approach [21, 22] also applied to estimate parameters of RBF-ARX models. Compared with general non-structured estimation methods, the SNPOM converges faster and more flexible, especially for the models whose number of linear parameters is much more than that of nonlinear parameters.

Following these parameter estimation methods, series of applications on RBF-ARX modeling have been done in recent years, including industrial application [10, 11], model-based predictive controller (MPC) design [13–16] and nonlinear time series prediction [19–22]. Although many efforts have been devoted to estimate the RBF-ARX models, till now, the studies mainly focus on the systems which are allowed to do identification experiments or easy to obtain the continuously changing identification data. However, there also exist a lot of actual industrial processes, which are not allowed to do the identification experiment in the actual production process or the dynamic characteristics of the processes strongly depend on the environment or working conditions. For this class of systems, such as the cut tobacco drying process, the historical data of once operation is not sufficient to contain the global dynamic characteristics of the process.

In this paper, considering this special industrial process identification problem, the multi-segment historical data set in different seasons and working conditions is used as identification data of the drying process models, and a hybrid optimization algorithm is designed to identify the MSR-Cubic-RBF-ARX model using the multi-segment historical data. To make the model have better long-term predictive capability to the head and tail stage drying process so as to achieve optimal setting control, a long-term forecasting performance index is introduced in the hybrid algorithm. As regards the convergence rate of the hybrid algorithm, a fundamental issue is a proper choice of the initial model parameters, which may make the optimization process quickly convergent. To accelerate the computational convergence, in the hybrid algorithm, we first minimize one-step predictive errors of the model to estimate the MSR-Cubic-RBF-ARX model parameters, which are only used as the model initial parameters, and then, we further optimize the model parameters by minimizing long-term forecasting errors of the model. This approach may significantly improve the optimization convergence rate, especially for the MSR-Cubic-RBF-ARX model, which has more linear parameters and fewer nonlinear parameters. The hybrid optimization process is given as follows.

Without loss of generality, the parameters of RBF-ARX model (3) can be divided into the linear parameters $\boldsymbol{\theta}_L = \left\{ c_k^y, c_{i,k}^y : i=1,\ldots,k_a; \ c_{i,k}^u : i=1,\ldots,k_b \middle| \ k=0,1,\ldots,m \right\}$ and nonlinear parameters $\boldsymbol{\theta}_N = \left\{ z_k^j \middle| k=1,\ldots,m; \ j=y,u \right\}$, and it is true to MSR-Cubic-RBF-ARX model (4) or (6). Taking the head stage process for example, the parameters of MSR-Cubic-RBF-ARX model (4) can be also divided into the linear parameters $\boldsymbol{\theta}_L^h = \{ c_k^{y^h}, c_{i,k}^{y^h} : i=1,\ldots,k_a^h; \ c_{i,k}^{u_\delta^h} : i=1,\ldots,k_b^h; \ |k=0,1,\ldots,m^h; \ \delta=1,2,3,4,5 \}$ and nonlinear parameters $\boldsymbol{\theta}_N^h = \left\{ z_{k,g}^{j,1}, z_{k,g}^{j,2} \middle| \ k=1,\ldots,m^h; \ j=y^h, u^h; \ g=1,\ldots,d^h \right\}$. Then, model (3), (4) or (6) can be rewritten in the following form:

$$y(t) = f(\boldsymbol{\theta}_L, \boldsymbol{\theta}_N, w(t-1))^T + \xi(t) \qquad (8)$$

or

$$y(t) = \varphi(\boldsymbol{\theta}_N, w(t-1))^T \boldsymbol{\theta}_L + \xi(t) \qquad (9)$$

Model (9) is the linear regression form of model (8) with respect to $\boldsymbol{\theta}_L$.

1. Modified SNPOM (M-SNPOM) algorithm

For making use of M-segment identification data, first, a modified SNPOM minimizing one-step-ahead predictive errors of the model is utilized to estimate the RBF-ARX model's parameters that will be used as the initial parameters of the model for further optimization. Objective function of the M-SNPOM is to take the sum of squares of the model one-step predictive residuals for M-segment identification data as follows:

$$V(\boldsymbol{\theta}_N, \boldsymbol{\theta}_L) \triangleq \sum_{p=1}^{M} \left(\frac{1}{2} \|\mathbf{F}^p(\boldsymbol{\theta}_N, \boldsymbol{\theta}_L)\|_2^2 \right) \qquad (10)$$

$$\begin{cases} \mathbf{F}^p(\boldsymbol{\theta}_N, \boldsymbol{\theta}_L) = \begin{bmatrix} \hat{y}^p(\tau+1|\tau) - \bar{y}^p(\tau+1) \\ \hat{y}^p(\tau+2|\tau+1) - \bar{y}^p(\tau+2) \\ \vdots \\ \hat{y}^p(n_p|n_p-1) - \bar{y}^p(n_p) \end{bmatrix}, \\ \hat{y}^p(t+1|t) = \sum_{i=1}^{k_a} a_{i,t}^p \bar{y}^p(t+1-i) + \sum_{i=1}^{k_b} b_{i,t}^p \bar{u}^p(t+1-i) + a_{0,t}^p \\ \qquad\qquad = \varphi(\boldsymbol{\theta}_N, \bar{w}^p(t-1))^T \boldsymbol{\theta}_L, \\ p=1,\ldots,M. \end{cases}$$

$$(11)$$

where $\left\{ \hat{y}^p(t+1|t) \middle| t=\tau, \tau+1,\ldots,n_p-1 \right\}$ is the RBF-ARX model (3)-based one-step-ahead prediction output for the pth-segment measured data; $\left\{ \bar{y}^p(j), \bar{w}^p(j) \middle| j=1,2,\ldots,n_p \right\}$ is the measured data in the pth-segment identification data set;

$\tau = \max(k_a, k_b)$ is the largest time lag of variables in model (3); n_p is the number of the pth-segment identification data. Optimization problem of the M-SNPOM is to compute

$$\left(\hat{\theta}_N, \hat{\theta}_L\right) = \arg\min_{\boldsymbol{\theta}_N, \boldsymbol{\theta}_L} V(\boldsymbol{\theta}_N, \boldsymbol{\theta}_L) \tag{12}$$

In the M-SNPOM, the optimization calculation centers on the search for $\boldsymbol{\theta}_N^{k+1}$ at the kth iteration step, followed by the immediately update of the linear parameters $\boldsymbol{\theta}_L^{k+1}$ using the LSM as follows: where $\{\bar{\mathbf{y}}^p | p = 1, \ldots, M\}$ is the pth-segment historical data; $\mathbf{R}(\boldsymbol{\theta}_N^{k+1})^+$ is the pseudo-inverse of $\mathbf{R}(\boldsymbol{\theta}_N^{k+1})$, which can be calculated using the singular value decomposition (SVD) for overcoming the ill-conditioned problems.

The innovative strategy of the nonlinear parameters $\boldsymbol{\theta}_N^k$ is as follows:

$$\boldsymbol{\theta}_L^{k+1} = \mathbf{R}(\boldsymbol{\theta}_N^{k+1})^+ \overline{\mathbf{Y}} \tag{13}$$

$$
\begin{cases}
\mathbf{R}(\boldsymbol{\theta}_N^{k+1})^+ = \left[\mathbf{R}(\boldsymbol{\theta}_N^{k+1})^{\mathrm{T}} \mathbf{R}(\boldsymbol{\theta}_N^{k+1})\right]^{-1} \mathbf{R}(\boldsymbol{\theta}_N^{k+1})^{\mathrm{T}}, \\
\mathbf{R}(\boldsymbol{\theta}_N^{k+1}) = \begin{pmatrix} \mathbf{r}^1(\boldsymbol{\theta}_N^{k+1}) \\ \mathbf{r}^2(\boldsymbol{\theta}_N^{k+1}) \\ \vdots \\ \mathbf{r}^M(\boldsymbol{\theta}_N^{k+1}) \end{pmatrix}, \quad \mathbf{r}^p(\boldsymbol{\theta}_N^{k+1}) = \begin{pmatrix} \varphi\left(\boldsymbol{\theta}_N^{k+1}, \bar{w}^p(\tau)\right)^T \\ \varphi\left(\boldsymbol{\theta}_N^{k+1}, \bar{w}^p(\tau+1)\right)^{\mathrm{T}} \\ \vdots \\ \varphi\left(\boldsymbol{\theta}_N^{k+1}, \bar{w}^p(n_p-1)\right)^{\mathrm{T}} \end{pmatrix}, \\
\overline{\mathbf{Y}} = (\bar{\mathbf{y}}^1, \bar{\mathbf{y}}^2, \ldots, \bar{\mathbf{y}}^M)^{\mathrm{T}}, \quad \bar{\mathbf{y}}^p = (\bar{y}^p(\tau+1), \quad \bar{y}^p(\tau+2), \ldots, \bar{y}^p(n_p)), \\
p = 1, \ldots, M.
\end{cases} \tag{14}
$$

$$\boldsymbol{\theta}_N^{k+1} = \boldsymbol{\theta}_N^k + \beta_k \mathbf{d}_k \tag{15}$$

where $\mathbf{d}_k$ is the search direction and k denotes the iteration step; β_k is the scalar step length parameter which reduces the distance to its minimum. In order to improve the robustness of the optimization process, based on the LMM algorithm, $\mathbf{d}_k$ in Eq. (15) can be obtained from a solution of the set of linear equations:

$$
\begin{aligned}
&[\mathbf{J}(\boldsymbol{\theta}_N^k)^{\mathrm{T}} \mathbf{J}(\boldsymbol{\theta}_N^k) + \gamma_k \mathbf{I}]\mathbf{d}_k = -\mathbf{J}(\boldsymbol{\theta}_N^k)^{\mathrm{T}} \mathbf{F}(\boldsymbol{\theta}_N^k, \boldsymbol{\theta}_L^k), \\
&\mathbf{F}(\boldsymbol{\theta}_N^k, \boldsymbol{\theta}_L^k) = (\mathbf{F}^1(\boldsymbol{\theta}_N^k, \boldsymbol{\theta}_L^k), \mathbf{F}^2(\boldsymbol{\theta}_N^k, \boldsymbol{\theta}_L^k), \ldots, \mathbf{F}^M(\boldsymbol{\theta}_N^k, \boldsymbol{\theta}_L^k))^{\mathrm{T}}.
\end{aligned} \tag{16}
$$

where $\mathbf{J}(\boldsymbol{\theta}_N^k)$ is the Jacobian matrix of $\mathbf{F}(\boldsymbol{\theta}_N^k, \boldsymbol{\theta}_L^k)$ with respect to $\boldsymbol{\theta}_N^k$, and the scalar γ_k can be used to control both the direction and the magnitude of $\mathbf{d}_k$. When γ_k tends to infinity, the search direction $\mathbf{d}_k$ will tend toward the steepest descent direction. As γ_k tends to zero, the search direction $\mathbf{d}_k$ will tend toward the Gauss–Newton direction. β_k in Eq. (15) is then calculated by a line search procedure, such as the mixed polynomial interpolation or extrapolation method.

The optimization termination condition is

$$V(\boldsymbol{\theta}_N^k, \boldsymbol{\theta}_L^k) - V(\boldsymbol{\theta}_N^{k+1}, \boldsymbol{\theta}_L^{k+1}) \leq \varepsilon \tag{17}$$

where ε is a given small positive number.

2. Modified-LMM (M-LMM) algorithm

After getting the initial parameters of model (3) by M-SNPOM, the model parameters are further optimized by minimizing long-term forecasting errors of the model using the M-LMM based on multi-segment identification data. Objective function of the M-LMM algorithm is to take the sum of squares of the model's long-term forecasting residuals for M-segment identification data as follows.

$$\bar{V}(\boldsymbol{\theta}_N, \boldsymbol{\theta}_L) \triangleq \sum_{p=1}^{M} \left(\frac{1}{2} \left\| \bar{\mathbf{F}}^p(\boldsymbol{\theta}_N, \boldsymbol{\theta}_L) \right\|_2^2\right) \tag{18}$$

$$
\begin{cases}
\bar{\mathbf{F}}^p(\boldsymbol{\theta}_N, \boldsymbol{\theta}_L) = \begin{bmatrix} \hat{y}^p(\tau+1|\tau) - \bar{y}^p(\tau+1) \\ \hat{y}^p(\tau+2|\tau) - \bar{y}^p(\tau+2) \\ \vdots \\ \hat{y}^p(n_p|\tau) - \bar{y}^p(n_p) \end{bmatrix}, \\
p = 1, \ldots, M.
\end{cases} \tag{19}
$$

where $\left\{\hat{y}^p(\tau+j|\tau) | j = 1, 2, \ldots, n_p - \tau\right\}$ is the model (3)-based $j(j = 1, 2, \ldots, n_i - \tau)$-step-ahead prediction of output for the pth-segment measured data at time τ.

From model (3), one can obtain the one-step-ahead prediction output $\hat{y}^p(\tau+1|\tau)$ at time τ as follows

$$
\begin{aligned}
\hat{y}^p(\tau+1|\tau) &= a_{0,\tau}^p + \sum_{i=1}^{k_n} a_{i,\tau}^p \bar{y}^p(\tau+1-i) \\
&+ \sum_{i=1}^{k_n} b_{i,\tau}^p \bar{u}^p(\tau+1-i)
\end{aligned} \tag{20}
$$

and the $j(j = 1, 2, \ldots, n_i - \tau)$-step-ahead predictive output $\hat{y}^i(\tau+j|\tau)$ can be also derived from model (3) as follows

$$\hat{y}^p(\tau + j|\tau) = a_{0,\tau+j-1|\tau}^p + \sum_{i=1}^{k_n} a_{i,\tau+j-1|\tau}^p \hat{y}^p(\tau + j - i|\tau)$$

$$+ \sum_{i=1}^{k_n} b_{i,\tau+j-1|\tau}^p \bar{u}^p(\tau + j - i) \qquad (21)$$

where

$$\begin{cases} \hat{y}^p(\tau + j - i|\tau) = \bar{y}^p(\tau + j - i), j \le i; \\ a_{0,\tau+j-1|\tau}^p = c_0^y + \sum_{k=1}^{m} c_k^y \varphi\left(\left\|\hat{w}^p(\tau + j - 1|\tau) - z_k^y\right\|_2\right), \\ a_{i,\tau+j-1|t}^p = c_{i,0}^y + \sum_{k=1}^{m} c_{i,k}^y \varphi\left(\left\|\hat{w}^p(\tau + j - 1|\tau) - z_k^y\right\|_2\right), \\ b_{i,\tau+j-1|t}^p = c_{i,0}^u + \sum_{k=1}^{m} c_{i,k}^u \varphi\left(\left\|\hat{w}^p(\tau + j - 1|\tau) - z_k^u\right\|_2\right). \end{cases}$$

$$(22)$$

Optimization problem of the M-LMM algorithm is to compute

$$\left(\hat{\theta}_N, \hat{\theta}_L\right) = \arg\min_{\theta_N, \theta_L} \bar{V}(\theta_N, \theta_L) \qquad (23)$$

and the parameters θ_N and θ_L of the RBF-ARX model are optimized by using the LMM algorithm [24] starting the initial parameters estimated by the M-SNPOM. Optimization termination condition in the M-LMM is

$$\bar{V}(\theta_N^k, \theta_L^k) - \bar{V}(\theta_N^{k+1}, \theta_L^{k+1}) \le \sigma \qquad (24)$$

where σ is a given small positive number.

There are some criterions that may be used to determine orders of the RBF-ARX models, such as Akaike information criterion (AIC) and Akaike Final Prediction Error (AFPE) [23]. In this paper, we use the AIC value as evaluation standard [9] to determine the RBF-ARX model orders (k_a, k_b, m and d), and simultaneously the dynamic characteristics of step response of the estimated model are also synthetically considered for finally obtaining a suitable model. By repetitively training the RBF-ARX model with different orders, the finally selected model should have small AIC value and well dynamic response characteristics.

3 MSR-Cubic-RBF-ARX model-based optimal setting control

After getting a proper MSR-Cubic-RBF-ARX model that has good long-term pretictive accuracy for the head or tail stage drying process, we can design a set of optimal setting variables to the drying process on the basis of the model to make over-dried cut tobacco in the head and tail stages of the drying process as few as possible. Considering the

different process property of the head stage and tail stage drying processes and the actual manual control experience, this paper designed different type of function curve as basic structure of the process variables, and based on the estimated process models, a set of optimal setting variables are obtained by optimizing parameters of the setting variable curves in this section.

3.1 Optimal setting control in head stage drying process

The input variables requiring optimal setting in the head drying stage are: the moisture exhaust opening, the hot air temperature, the cylinder temperature and the inlet cut tobacco flow, to make the outlet cut tobacco moisture content can rise to the set value as quick as possible, and the over-dried cut tobacco can be reduced as much as possible. Gradient of middle part of the S-type function is the largest, but in the first half process of the head stage the cut tobacco volume-in-dryer is fewer, so the cylinder temperature etc. cannot be increased too quickly in the case; therefore, we designed the double-S-type function as the optimal setting curves of the moisture exhaust opening, the hot air temperature and the cylinder temperature and a T-type function as the inlet cut tobacco flow optimal setting curve in the head stage. The actual manual operating experience also verified this design.

The double-S function-type setting curves of the moisture exhaust opening, the hot air temperature and the cylinder temperature are $Df_{u_1^h}(t)$, $Df_{u_2^h}(t)$ and $Df_{u_3^h}(t)$, respectively, which are as follows:

$$Df_{u_i^h}(t) = \frac{\lambda_1^i}{1 + e^{-\frac{t-\lambda_2^i}{\lambda_3^i}}} + \lambda_4^i + \frac{\lambda_5^i}{1 + e^{-\frac{t-\lambda_6^i}{\lambda_7^i}}}, \quad i = 1, 2, 3 \quad (25)$$

where t is the time-point; $\{\lambda_1^i, \lambda_4^i, \lambda_5^i | i = 1, 2, 3\}$ are parameters which are used to decide the start point, switching point and end point of the double-S function-type curve; $\{\lambda_2^i, \lambda_6^i | i = 1, 2, 3\}$ decide the symmetry axis; $\{\lambda_3^i, \lambda_7^i | i = 1, 2, 3\}$ decide the rising or falling speed of the double-S function-type curve. The T-type function setting value of the inlet cut tobacco flow is taken as follows:

$$Tf_{u_4^h}(t) = \begin{cases} \frac{k_1 t}{k_2}, & 1 \le t \le k_2 \\ k_1, & k_2 + 1 \le t \le k_3 \\ k_1 - \frac{(k_1 - k_5)(t - k_3)}{k_4 - k_3}, & k_3 + 1 \le t \le k_4 \\ k_5, & k_4 + 1 \le t \le M^h \end{cases}$$

$$(26)$$

where k_1, k_2, k_3, k_4, k_5 are the related parameters of the T-type function curve.

By substituting setting curves (25)–(26) into MSR-Cubic-RBF-ARX model (4), one can get the predictive outlet cut tobacco moisture content value in the head drying stage as follows

$$\hat{y}^h(t) = f\left(Df_{u_1^h}, Df_{u_2^h}, Df_{u_3^h}, Tf_{u_4^h}\right) \qquad (27)$$

Error between the predictive outlet cut tobacco moisture content value (27) and the desired output value $y_r^h(t)$ is defined as:

$$e^h(t) = y_r^h(t) - \hat{y}^h(t) \qquad (28)$$

By minimizing the error using the LMM algorithm [24], one can find out the optimal parameters $\left\{\lambda_j^i | i = 1, 2, 3; \quad j = 1, \ldots, 7\right\}$ and $\left\{k_g | g = 1, \ldots, 3\right\}$ in (25) and (26). This can be done by solving the following optimization problem using LMM:

$$\min_{\lambda_j^i, k_g} J = \sum_{t=1}^{M^h} \left(e^h(t)\right)^2 \qquad (29)$$

where M^h is duration time of the head drying stage. The optimization results are showed in Sect. 4.

3.2 Optimal setting control in tail stage drying process

The input variables requiring optimal setting in the tail drying stage are: the moisture exhaust opening, the hot air temperature, the cylinder temperature and the cylinder motor frequency, to make the outlet cut tobacco moisture content can be kept at the set value as long as possible, and the over-dried cut tobacco can be reduced as much as possible. In the tail stage, the cut tobacco volume-in-dryer will decrease to zero, and the cylinder temperature etc. needs to vary quickly in the case, so the S-type setting curves are better for the tail stage. The actual manual operating experience also verified this design. The following S-type function is designed as the optimal setting curves of the four input variables, which are $Sf_{u_1^e}(t)$, $Sf_{u_2^e}(t)$, $Sf_{u_3^e}(t)$ and $Sf_{u_4^e}(t)$, respectively,

$$Sf_{u_1^e}(t) = \frac{x_1^i}{1 + e^{-\frac{t - x_2^i}{x_3^i}}} + x_4^i, \quad i = 1, 2, 3, 4. \qquad (30)$$

where $\left\{x_j^i | i = 1, 2, 3, 4; \quad j = 1, 2, 3, 4\right\}$ are the related parameters of the S-type function curves.

By substituting setting curves (30) into MSR-Cubic-RBF-ARX model (6), one can get the predictive outlet cut tobacco moisture content value in the tail drying stage as follows

$$\hat{y}^e(t) = f\left(Sf_{u_1^e}, Sf_{u_2^e}, Sf_{u_3^e}, Sf_{u_4^e}\right) \qquad (31)$$

Error between the predictive outlet cut tobacco moisture content value (31) and the desired output value $y_r^e(t)$ is defined as:

$$e^e(t) = y_r^e(t) - \hat{y}^e(t) \qquad (32)$$

By minimizing the error using the LMM algorithm [24], one can find out the optimal parameters $\left\{x_j^i | i = 1, 2, 3, 4; \quad j = 1, 2, 3, 4\right\}$ in (30). This can be done by solving the following optimization problem using LMM:

$$\min_{\alpha_{i,j}} J = \sum_{t=1}^{M^e} \left(e^e(t)\right)^2 \qquad (33)$$

where M^e is the duration time of the tail drying stage. The optimization results are showed in Sect. 4.

4 Simulation studies

In this section, the proposed MSR-Cubic-RBF-ARX modeling and setting control strategy are applied to the head and tail stage drying process of an actual cylinder-type cut tobacco dryer for simulation studies. Considering that the outlet cut tobacco moisture content in the drying process is influenced by many factors such as environment humidity and temperature, as well as machine working conditions, the real-time sampled multi-segment historical data in different seasons and working conditions depicted in Figs. 2 and 3 are used as identification data of the drying process model, and then, the proposed hybrid optimization algorithm is applied to identify the MSR-Cubic-RBF-ARX models using the multi-segment identification data.

Figure 2 shows 12-segment actual historical data of the head stage drying process, and the data of each segment last 600 s. The sampling period of the drying process is 1 s, and there are 7200 sampling data points totally. In this paper, the first 6-segment historical data are used to train MSR-Cubic-RBF-ARX model (4) of the head stage drying process, and the last 6-segment data are used to test the modeling performance. Figure 3 shows 12-segment actual historical data of the tail stage drying process, and each segment lasts 800 s. There are 9600 sampling data points totally. The first 6-segment historical data are used to train MSR-Cubic-RBF-ARX model (6) of the tail stage process, and the last 6-segment data are used to test the modeling performance.

4.1 MSR-Cubic-RBF-ARX model identification results

By applying the hybrid optimization algorithm and the model evaluation standard presented in Sect. 2.2, after
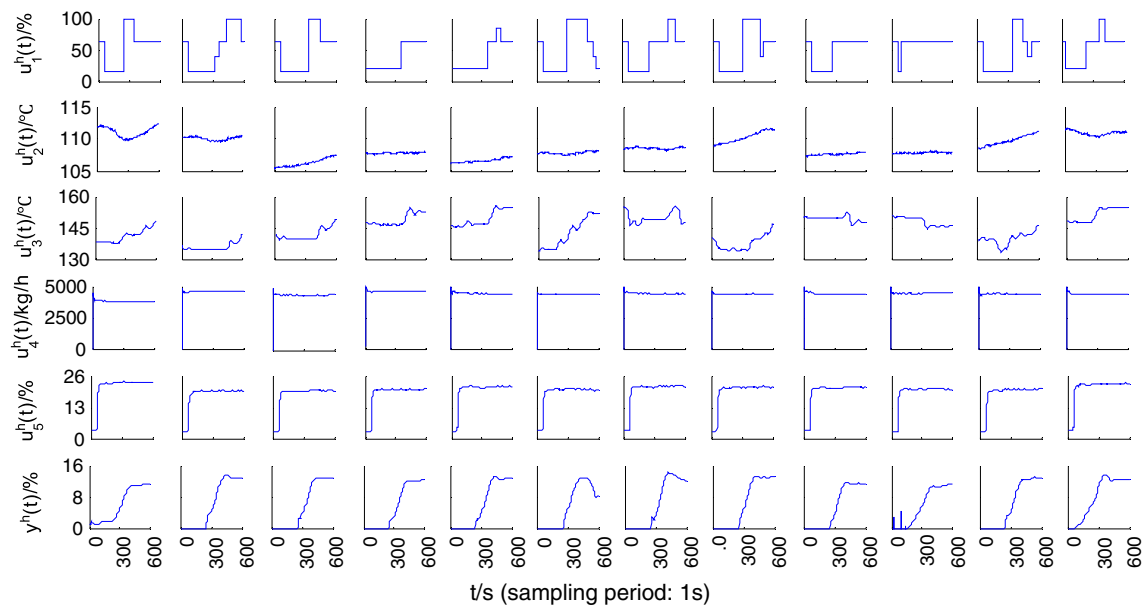
Fig. 2 Identification data of MSR-Cubic-RBF-ARX model (4) in head stage drying process
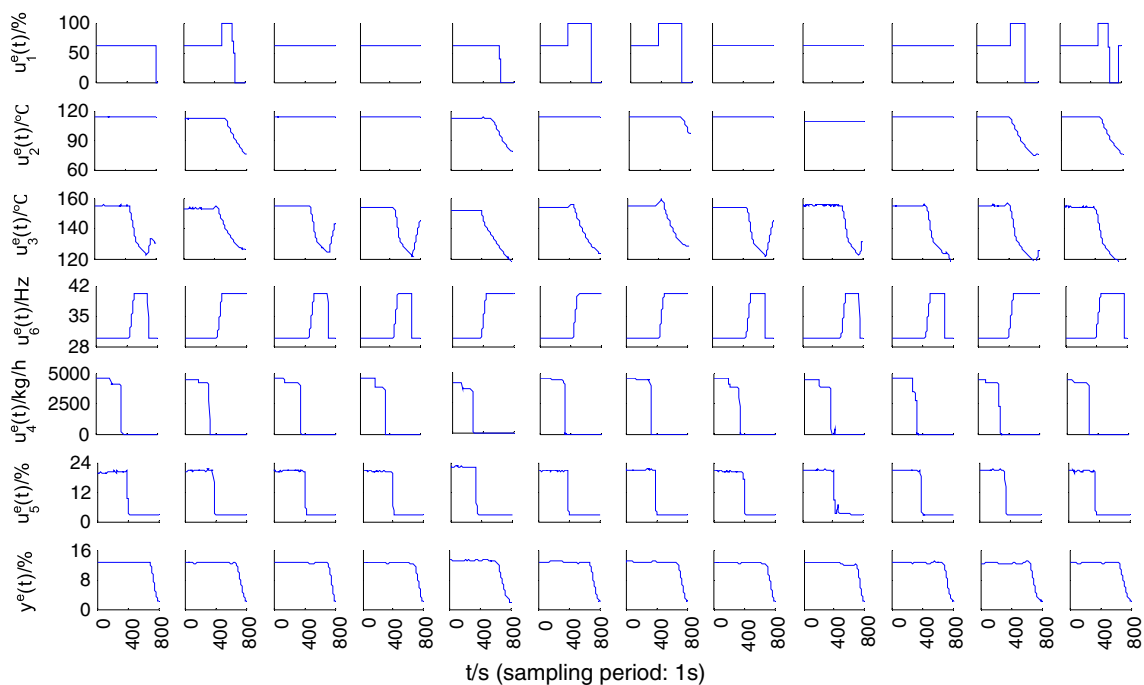

**Fig. 3** Identification data of MSR-Cubic-RBF-ARX model (6) in tail stage drying process

repetitively training and comparison, orders of MSR-Cubic-RBF-ARX models of the cut tobacco drying process are finally determined as: $k_a^h = 2$, $k_b^h = 30$, $m^h = 2$, $d^h = 4(2, 30, 2, 4)$ for the head stage, and $k_a^e = 1$, $k_b^e = 12$, $m^e = 2$, $d^e = 7(1, 12, 2, 7)$ for the tail stage. Moreover, the measurable time delay orders of MSR-Cubic-RBF-ARX models of the drying process are: $T_1^h = 60$, $T_2^h = 10$, $T_3^h = 200$ for the head stage and $T_1^e = 60$, $T_2^e = 120$, $T_3^e = 190$

for the tail stage. The corresponding modeling results for the 6-segment training or testing data are depicted in Figs. 4 and 5.

It is natural that the ability of multi-step-ahead forecasting is an important evaluating indicator for nonlinear system modeling. Figures 4 and 5 show the actual output (blue line), the multi-step-ahead predicted output (red line) generated by the estimated MSR-
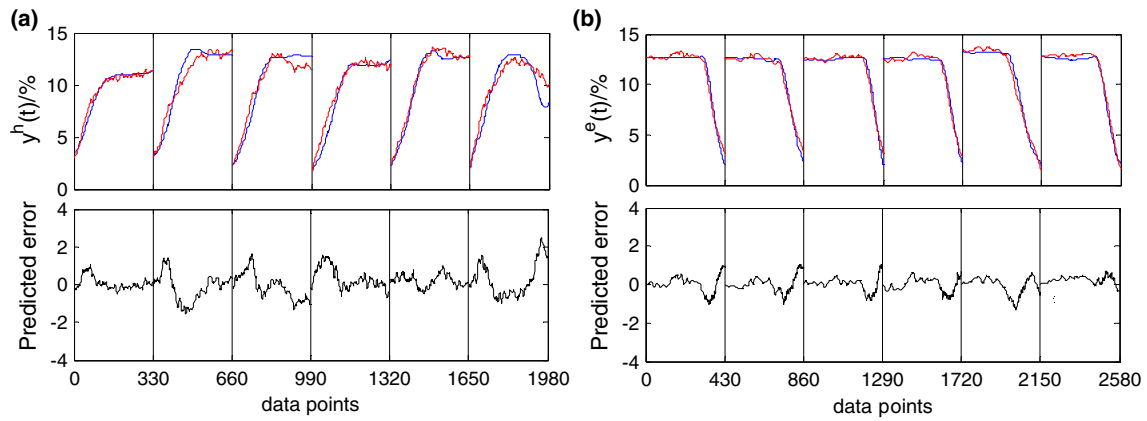
Fig. 4 Outputs and multi-step-ahead predicted errors of multi-sampling-rate Cubic-RBF-ARX models for 6-segment training data. **a** Identification results for head stage drying process. **b** Identification results for tail stage drying process
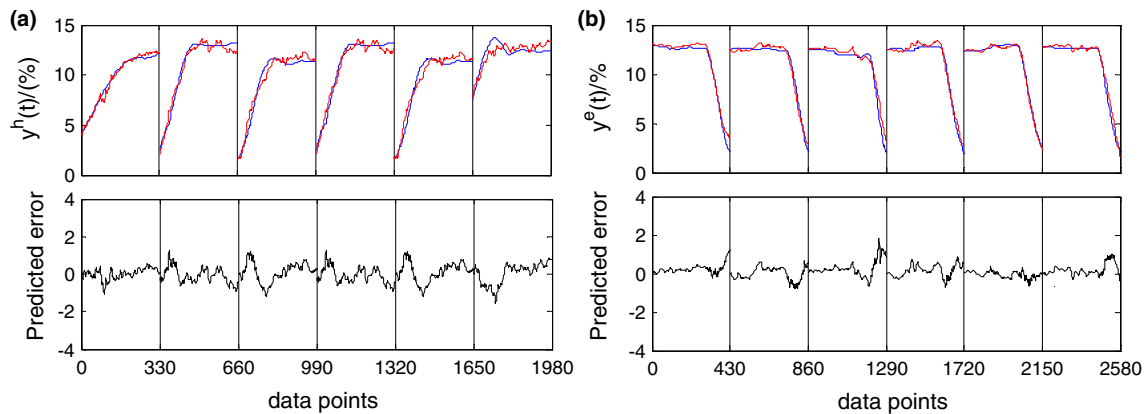
Fig. 5 Outputs and multi-step-ahead predicted errors of multi-sampling-rate Cubic-RBF-ARX models for 6-segment testing data. **a** Identification results for head stage drying process. **b** Identification results for tail stage drying process

Cubic-RBF-ARX model and the multi-step-ahead predicted errors for the head and tail stages, respectively. From Figs. 4 and 5, one can see that the output of the estimated MSR-Cubic-RBF-ARX model is very close to the actual output, and the long-term prediction errors are between $+2$ and -2 only for these quickly varying data. This demonstrates that the multi-sampling-rate Cubic-RBF-ARX model identified by the proposed hybrid optimization algorithm for the head and tail stage drying process modeling possesses very good long-term forecasting accuracy.

4.2 MSR-RBF-ARX modeling results with different base functions

In the modeling, evaluation of various base functions contributes to selection of optimal structure of the MSR-RBF-ARX model. In this paper, the potential base functions used in the MSR-RBF-ARX model for the head and tail stage drying process modeling include:

1. Gauss function:

$$\varphi(r) = \exp\left(-\frac{r^2}{2\sigma^2}\right) \quad \sigma > 0, \quad r \in \Re. \tag{34}$$

2. Cubic function:

$$\varphi(r) = r^3 \quad r \in \Re. \tag{35}$$

3. Multiquadratic function:

$$\varphi(r) = (r^2 + \sigma^2)^{1/2} \quad \sigma > 0, r \in \Re. \tag{36}$$

To fairly compare three types of MSR-RBF-ARX models with Gauss, Cubic and Multiquadratic base function, respectively, we use the proposed hybrid optimization algorithm to estimate their parameters and use the same way presented in Sect. 2.2 to determine the models orders. In this paper, we use the mean square error (MSE) that is the most commonly used relative quality measure to

Table 1 AIC values and MSE values of MSR-RBF-ARX models with different base function

Model (k_a, k_b, m, d)	AIC	MSE
Head stage		
Gaussian-(3,28,2,5)	-1.6958×10^4	3.6236×10^3
Cubic-(2,30,2,4)	$\mathbf{-1.9721 \times 10^4}$	$\mathbf{3.3343 \times 10^3}$
Multiquadratic-(4,24,1,9)	-1.5775×10^4	4.8324×10^3
Tail stage		
Gaussian-(2,15,1,8)	-3.0652×10^4	1.0878×10^4
Cubic-(1,12,2,7)	$\mathbf{-3.1359 \times 10^4}$	$\mathbf{9.9445 \times 10^3}$
Multiquadratic-(4,18,2,7)	-3.0031×10^4	1.8259×10^4
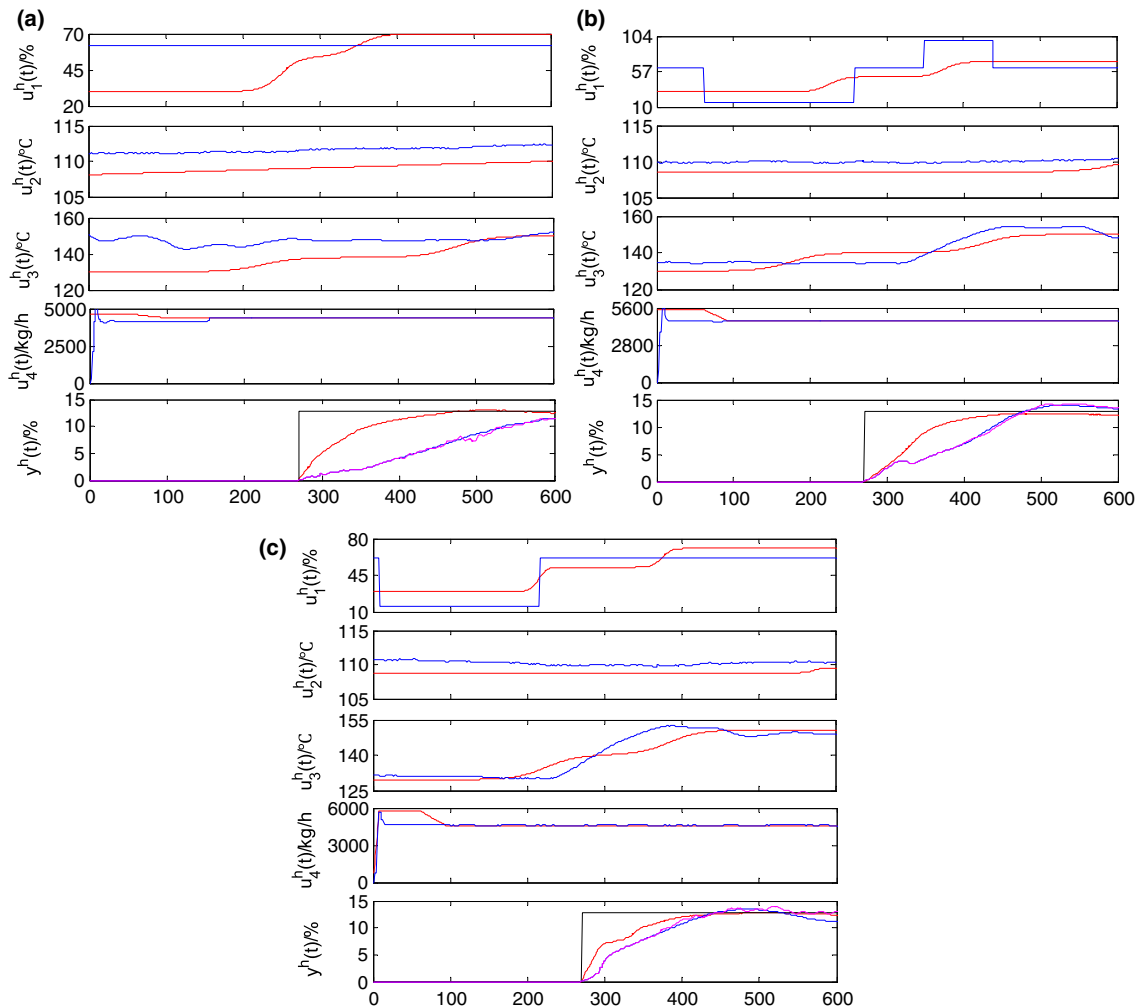
Fig. 6 Simulation results of optimal setting control of head stage drying process in different working conditions

statistical models [25] to evaluate the modeling performance, which is defined as follows:

$$\text{MSE} = \frac{\sum_{t=\tau}^{N_t}(y(t) - \hat{y}(t))^2}{N_t} \qquad (37)$$

where $y(t)$ is the actual output and $\hat{y}(t)$ is the long-term forecasting output of a model, τ is the largest time lag of variables in model; N_t is the number of identification data.

Using the data in Figs. 2 and 3, modeling results of the MSR-RBF-ARX models with the three types of base functions above are shown in Table 1.

From Table 1, one can see that the MSR-RBF-ARX model with Cubic base function produces smaller AIC and MSE than other two models with other base function no matter for the head or tail stage drying process modeling. The results indicate that the multi-sampling-rate RBF-ARX

model with Cubic base function can better represent the global characteristics of the head or tail stage drying process.

4.3 Optimal setting control simulation results

Simulation results of optimal setting control of the head stage drying process in different working conditions based on the MSR-Cubic-RBF-ARX model estimated in Sect. 4.1 are shown in Fig. 6. The upper four subplots in Fig. 6a–c show the four input control variables (moisture exhaust opening, hot air temperature, cylinder temperature and inlet cut tobacco flow) in the head stage drying process, in which the blue lines are actual input variables, and the red lines are optimal setting curves of the input variables by optimization presented in Sect. 3. The bottom subplot of Fig. 6a–c shows the outlet cut tobacco moisture content, in which the black line is the desired value, the blue line is the actual value, the red line is the MSR-Cubic-RBF-ARX model output under the red optimal setting inputs above and the pink line shows the long-term predicted outputs generated by the estimated MSR-Cubic-RBF-ARX model (4) using the actual input signals.

In optimal setting control of the head stage, the optimization duration time is set as $M^h=600$ s. Finally, the optimized double-S-type setting functions of moisture exhaust opening, hot air temperature and cylinder temperature in Fig. 6a are $Sf_{u_1^s}(t) = \frac{24}{1+e^{-\frac{t-250}{11.9749}}} + 30 + \frac{16}{1+e^{-\frac{t-350}{15}}}$, $Sf_{u_2^s}(t) = \frac{13.1988}{1+e^{-\frac{t+96.171}{999}}} + 101.1799$ and $Sf_{u_3^s}(t) = \frac{8}{1+e^{-\frac{t-225}{22}}} + 130 + \frac{12}{1+e^{-\frac{t-475}{22}}}$, respectively. The optimized T-type setting function of inlet cut tobacco flow in Fig. 6a is

$$Tf_{u_4^s}(t) = \begin{cases} 4600, & 1 \le t \le 60 \\ 4600 - \frac{100(t-60)}{17}, & 61 \le t \le 94 \\ 4400, & 95 \le t \le 600 \end{cases} \quad (38)$$

In Fig. 6b, the optimized double-S-type setting functions are $Sf_{u_1^s}(t) = \frac{20}{1+e^{-\frac{t-225}{10}}} + 30 + \frac{20}{1+e^{-\frac{t-375}{10}}}$, $Sf_{u_2^s}(t) = \frac{2.8575}{1+e^{-\frac{t-612.7771}{26.2348}}} + 108.55$ and $Sf_{u_3^s}(t) = \frac{10}{1+e^{-\frac{t-175}{20}}} + 130 + \frac{10}{1+e^{-\frac{t-425}{20}}}$, respectively. The optimized T-type setting function in Fig. 6b is

$$Tf_{u_4^s}(t) = \begin{cases} 5500, & 1 \le t \le 64 \\ 5500 - \frac{300(t-64)}{11}, & 65 \le t \le 97 \\ 4600, & 98 \le t \le 600 \end{cases} \quad (39)$$

In Fig. 6c, the optimized double-S-type setting functions are $Sf_{u_1^s}(t) = \frac{23.0619}{1+e^{-\frac{t-215}{5}}} + 29.5887 + \frac{18.0619}{1+e^{-\frac{t-375}{6}}}$, $Sf_{u_2^s}(t) = \frac{0.6382}{1+e^{-\frac{t-570.4686}{4.2970}}} + 108.8$ and $Sf_{u_3^s}(t) = \frac{10.5621}{1+e^{-\frac{t-225}{20}}} + 129.5885 + \frac{10.5621}{1+e^{-\frac{t-385}{20}}}$, respectively. The optimized T-type setting function in Fig. 6c is

$$Tf_{u_4^s}(t) = \begin{cases} \frac{5800t}{8}, & 1 \le t \le 8 \\ 5800, & 9 \le t \le 58 \\ 5800 - \frac{200(t-58)}{16}, & 59 \le t \le 91 \\ 4600, & 92 \le t \le 600 \end{cases} \quad (40)$$

From Fig. 6a–c, one can see that the rising speed of the optimized outlet cut tobacco moisture content is fast and has small overshoot on the basis of the Cubic-RBF-ARX model (4) with the double-S-type function and T-type function optimal setting inputs. It means that the over-dried cut tobacco in the head stage drying process will be greatly reduced. One can also see that the long-term predicted outputs of the Cubic-RBF-ARX models under the action of actual inputs are very close to the actual moisture content of outlet cut tobacco. This also indicates the good modeling accuracy of the Cubic-RBF-ARX model (4) to the head stage drying process.

Simulation results of optimal setting control of the tail stage drying process in different working conditions are shown in Fig. 7. The upper four subplots in Fig. 7a–c show the four input control variables (moisture exhaust opening, hot air temperature, cylinder temperature and cylinder motor frequency) in the tail stage process, in which the blue lines are actual input variables, and the red lines are optimal setting curves of the input variables by optimization presented in Sect. 3. The bottom subplot of Fig. 7a–c shows the outlet cut tobacco moisture content, in which the black line is the desired value, the blue line is the actual value, the red line is the MSR-Cubic-RBF-ARX model output under the red optimal setting inputs above and the pink line shows the long-term predicted outputs generated by the estimated MSR-Cubic-RBF-ARX model (6) using the actual input signals.

In Fig. 7a–c, the former 320 s signals show actual data of the middle stage drying process, after that optimal setting control of the tail stage process starts. The optimization duration time of the tail stage process is set as $M^e = 480$ s, and the maximum limit of the cylinder motor frequency is set as 44 (Hz). The optimized S-type setting functions of the moisture exhaust opening, hot air temperature, cylinder temperature and cylinder motor frequency in Fig. 7a are $Sf_{u_1^e}(t) = \frac{52}{1+e^{-\frac{t-300}{45}}} + 10$, $Sf_{u_2^e}(t) = \frac{34.17}{1+e^{-\frac{t-347.1}{35}}} + 79$, $Sf_{u_3^e}(t) = \frac{36.7}{1+e^{-\frac{t-213.4}{51}}} + 118.9$ and $Sf_{u_6^e}(t) = \frac{13}{1+e^{-\frac{t-310}{17.88}}} + 30$, respectively. In Fig. 7b, the optimized S-type setting functions are $Sf_{u_1^e}(t) = \frac{52}{1+e^{-\frac{t-134.4}{26.9}}} + 10$, $Sf_{u_2^e}(t) = \frac{33.6}{1+e^{-\frac{t-340.4}{35}}} + 79.1$, $Sf_{u_3^e}(t) = \frac{35.3}{1+e^{-\frac{t-174.8}{50}}} + 119$ and $Sf_{u_6^e}(t) = \frac{14}{1+e^{-\frac{t-345.8}{12}}} + 30$, respectively. In Fig. 7c, the
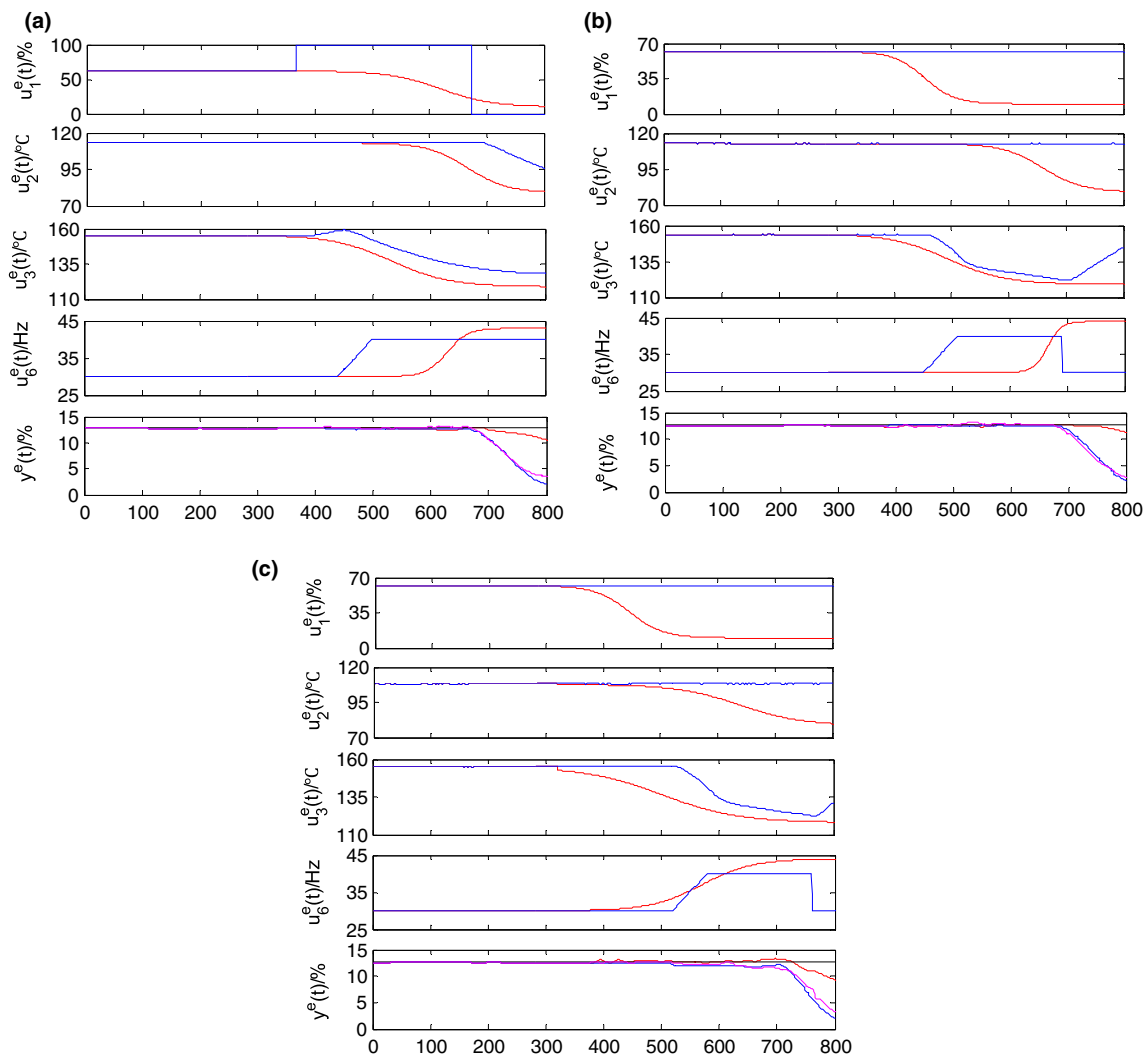
Fig. 7 Simulation results of optimal setting control of tail stage drying process in different working conditions

optimized S-type setting functions are $Sf_{u_1^e}(t) = \frac{52}{1+e^{\frac{t-125.6}{29.77}}} + 10$, $Sf_{u_2^e}(t) = \frac{29.2}{1+e^{\frac{t-319.3}{54.6}}} + 78.5$, $Sf_{u_3^e}(t) = \frac{36.9}{1+e^{\frac{t-182.7}{65.9}}} + 118$ and $Sf_{u_6^e}(t) = \frac{14}{1+e^{-\frac{t-250.5}{43.94}}} + 30$, respectively.

From Fig. 7a–c, it is clear that decline of the optimized outlet cut tobacco moisture content is largely deferred on the basis of Cubic-RBF-ARX model (6) with the S function-type optimal setting input curves. It means that the over-dried cut tobacco in the tail stage process can be greatly reduced. One can also see that the long-term predicted outputs of the Cubic-RBF-ARX models under the action of actual inputs are very close to the actual moisture content of outlet cut tobacco. This also indicates the good modeling accuracy of the Cubic-RBF-ARX model (6) to the tail stage drying process.

From the results in Figs. 6 and 7, it is verified that the optimal setting curves of input variables based on Cubic-

RBF-ARX model can make the outlet moisture content in the head stage more rapidly rise and reach the stable state and can make the outlet moisture content in the tail stage decline more slowly. Thus, over-dried cut tobacco in the head and tail stages can be greatly reduced using the proposed modeling and optimal setting control method.

5 Conclusions

Considering actual characteristics of the drying process of a cylinder-type cut tobacco dryer, a MSR-RBF-ARX model structure was designed and utilized for representing dynamic behavior of the head or tail stage drying process. Through comparison of several model structures, it was verified that the MSR-RBF-ARX model with Cubic function-type base function can better represent the global

characteristics of the head or tail stage drying process. For this special industrial process identification problem, the multi-segment historical data set in different seasons and working conditions were suitable to be used as identification data of the drying process models. A hybrid optimization algorithm was designed to identify the MSR-RBF-ARX model using multi-segment historical data. The modeling results indicated that the multi-sampling-rate Cubic-RBF-ARX models of the head and tail stage processes, which were identified by the hybrid optimization algorithm, achieved very good long-term forecasting accuracy. Based on the estimated MSR-Cubic-RBF-ARX model, sets of optimal setting input variables could be designed to implement optimal head or tail stage drying process control. Simulation results showed that the MSR-Cubic-RBF-ARX modeling and setting control strategy could make the outlet cut tobacco moisture content in head stage drying process quickly increase and reach stable state and also could make that in the tail stage drying process decrease more slowly. Thus, over-dried cut tobacco in the head and tail stage drying process could be greatly reduced.

References

1. Legros R, Alan Millington C, Clift R (1994) Drying of tobacco particles in a mobilised bed. Dry Technol 12(3):517–543
2. Wang H, Xin H, Liao Z, Li J, Xie W, Zeng Q, Li Y, Li Q, Chen X (2014) Study on the effect of cut tobacco drying on the pyrolysis and combustion properties. Dry Technol 32(2):130–134
3. Ludnev I (1996) Investigations on the technology of thermal and humidity treatment of tobacco. Presented at Cooperation Centre for Scientific Research Relative to Tobacco, Japan
4. Kiranoudis C, Maroulis Z, Marinos-Kouris D (1990) Mass transfer modeling for Virginia tobacco curing. Dry Technol 8(2):351–366
5. Pakowski Z, Druzdzel A, Drwiega J (2004) Validation of a model of an expanding superheated steam flash dryer for cut tobacco based on processing data. Dry Technol 22(1–2):45–57
6. Alvarez-López I, Llanes-Santiago O, Verdegay JL (2005) Drying process of tobacco leaves by using a fuzzy controller. Fuzzy Sets Syst 150(3):493–506
7. Ławryńczuk M (2011) Accuracy and computational efficiency of suboptimal nonlinear predictive control based on neural models. Appl Soft Comput 11(2):2202–2215
8. Nelles O (2013) Nonlinear system identification: from classical approaches to neural networks and fuzzy models. Springer Science & Business Media, Berlin
9. Peng H, Ozaki T, Haggan-Ozaki V, Toyoda Y (2003) A parameter optimization method for radial basis function type models. IEEE Trans Neural Netw 14(2):432–438
10. Haggan-Ozaki V, Ozaki T, Toyoda Y (2009) An Akaike state-space controller for RBF-ARX models. IEEE Trans Control Syst Technol 17(1):191–198
11. Peng H, Nakano K, Shioya H (2007) Nonlinear predictive control using neural nets-based local linearization ARX model-stability and industrial application. IEEE Trans Control Syst Technol 15(1):130–143
12. Peng H, Wu J, Inoussa G, Deng Q, Nakano K (2009) Nonlinear system modeling and predictive control using the RBF nets-based quasi-linear ARX model. Control Eng Pract 17(1):59–66
13. Zhou F, Peng H, Qin Y, Zeng X, Xie W, Wu J (2015) RBF-ARX model-based MPC strategies with application to a water tank system. J Process Control 34:97–116
14. Wu J, Peng H, Ohtsu K, Kitagawa G, Itoh T (2012) Ship's tracking control based on nonlinear time series model. Appl Ocean Res 36:1–11
15. Qin Y, Peng H, Ruan W, Wu J, Gao J (2014) A modeling and control approach to magnetic levitation system based on state-dependent ARX model. J Process Control 24(1):93–112
16. Wu J, Peng H, Chen Q, Peng X (2014) Modeling and control approach to a distinctive quadrotor helicopter. ISA Trans 53(1):173–185
17. Priestley M (1980) State-dependent models: a general approach to non-linear time series analysis. J Time Ser Anal 1(1):47–71
18. Harpham C, Dawson CW (2006) The effect of different basis functions on a radial basis function network for time series prediction: a comparative study. Neurocomputing 69(16):2161–2170
19. Gan M, Peng H, Chen L (2012) A global-local optimization approach to parameter estimation of RBF-type models. Inf Sci 197:144–160
20. Gan M, Peng H, X-p Dong (2012) A hybrid algorithm to optimize RBF network architecture and parameters for nonlinear time series prediction. Appl Math Model 36(7):2907–2915
21. Gan M, Li H-X, Peng H (2015) A variable projection approach for efficient estimation of RBF-ARX model. IEEE Trans Cybern 45(3):462–471
22. Gan M, Li H-X (2014) An efficient variable projection formulation for separable nonlinear least squares problems. IEEE Trans Cybern 44(5):707–711
23. Sadabadi MS, Shafiee M, Karrari M (2009) Two-dimensional ARMA model order determination. ISA Trans 48(3):247–253
24. Yamashita N, Fukushima M (2001) On the rate of convergence of the Levenberg–Marquardt method. In: Topics in numerical analysis. Springer, Vienna, pp 239–249
25. Xu Z, Chang X, Xu F, Zhang H (2012) Regularization: a thresholding representation theory and a fast solver. IEEE Trans Neural Netw Learn Syst 23(7):1013–1027